Journal of Biomolecular NMR, **26:** 167–179, 2003.
KLUWER/ESCOM

A novel strategy for the assignment of side-chain resonances in completely deuterated large proteins using ^{13}C spectroscopy

Alexander Eletsky[a], Osvaldo Moreira[a], Helena Kovacs[b] & Konstantin Pervushin[a,*]
[a]*Laboratory of Physical Chemistry, Swiss Federal Institute of Technology, ETH-Hönggerberg, CH-8093 Zürich, Switzerland;* [b]*Bruker BioSpin AG, Industriestrasse 26, CH-8117 Fällanden, Switzerland*

Received 3 February 2003; Accepted 24 February 2003

Abstract

The assignment of the aliphatic ^{13}C resonances of trimeric *Bacillus Subtilis* chorismate mutase, a protein with a molecular mass of 44 kDa, consisting of three 127-residue monomers is presented by use of two-dimensional (2D) ^{13}C-start and ^{13}C-observe NMR experiments. These experiments start with ^{13}C excitation and end with ^{13}C observation while relying on the long transverse relaxation times of ^{13}C spins in uniformly deuterated and ^{13}C,^{15}N-labeled large proteins. Gains in sensitivity are achieved by the use of a paramagnetic relaxation enhancement agent to reduce ^{13}C T_1 relaxation times with little effect on ^{13}C T_2 relaxation times. Such 2D ^{13}C-only NMR experiments circumvent problems associated with the application of conventional experiments for side-chain assignment to proteins of larger sizes, for instance, the absence or low concentration of the side-chain ^{1}H spins, the transfer of the side-chain spin polarization to the ^{1}H^N spins for signal acquisition, or the necessity of a quantitative reprotonation of the methyl moieties in the otherwise fully deuterated side-chains. We demonstrate that having obtained a nearly complete assignment of the side-chain aliphatic ^{13}C resonances, the side-chain ^{1}H chemical shifts can be assigned in a semiautomatic fashion using 3D ^{15}N-resolved and ^{13}C-resolved NOESY experiments measured with a randomly partially protonated protein sample. We also discuss perspectives for structure determination of larger proteins by using novel strategies which are based on the {^{1}H,^{1}H} NOEs in combination with multiple residual dipolar couplings between adjacent ^{13}C spins determined with 2D ^{13}C-only experiments.

Abbreviations: TROSY – transverse relaxation-optimized spectroscopy; 2D – two-dimensional; BsCM – 44 kDa enzyme chorismate mutase (EC 5.4.99.5) from *Bacillus subtilis*; RDC – residual dipole/dipole coupling.

Introduction

The general problem posed in 3D structure determination of biomolecules by NMR involves collection of a sufficiently dense set of experimental restraints to define the structure. These can be derived from interproton NOEs (Wüthrich, 1986; Ernst et al., 1987; Clore and Gronenborn 1991), residual dipole-dipole couplings and CSA interactions (Ernst and Ernst, 1994; Tolman et al., 1995; Tjandra and Bax, 1997; Tjandra et al., 1997b; Choy et al., 2001; Wu et al., 2001), scalar J couplings (Wüthrich, 1986; Bax, 1994), J couplings across-hydrogen bonds (Dingley and Grzesiek, 1998; Pervushin et al., 1998) and auto- and cross-correlated relaxation rates (Reif et al., 1997; Tjandra et al., 1997a). Currently available computer-based 3D structure reconstruction methods require that a large number of experimental restraints are assigned to particular atoms in the protein's chemical structure at the outset of structure determination (Clore and Schwieters, 2002). In large proteins this assignment problem is aggravated by the fast transverse relaxation of the spins of interest and the complexity of the NMR spectra, both of which increase with increasing molecular size (Wagner, 1993; Clore and Gronenborn, 1997, 1998; Kay and Gardner, 1997).

The use of TROSY (Pervushin et al., 1997) together with uniform deuteration (Browne et al., 1973; LeMaster, 1989; 1990a, b; Venters et al., 1997) re-

*To whom correspondence should be addressed. E-mail: kopeko@phys.chem.ethz.ch

duces transverse relaxation rates of $^{1}H^{N}$, ^{15}N and ^{13}C spins enabling successful assignment of the backbone resonances in large soluble protein complexes (Salzmann et al., 2000; Takahashi et al., 2000; Tugarinov et al., 2002) and integral membrane proteins solubilized in micelles (Arora and Tamm, 2001; Fernandez et al., 2001a, b; Hwang et al., 2002; Schubert et al., 2002). The uniform deuteration together with triple resonance experiments for backbone resonance assignment was first demonstrated by the NIH group (Grzesiek et al., 1993). Side-chain ^{13}C chemical shifts in fully perdeutared proteins can be correlated with the $^{1}H^{N}$ and ^{15}N chemical shifts using experiments starting with ^{13}C magnetization and detecting $^{1}H^{N}$ (Farmer and Venters, 1996; Lohr and Ruterjans 2002). Although ^{13}C transverse relaxation in ^{13}C-^{2}H moieties is expected to be 6 times slower than in ^{13}C-^{1}H moieties, relaxational losses associated with the use of long in-phase magnetization transfer periods from $^{13}C'$ or $^{13}C^{\alpha}$ to ^{15}N can reduce the efficiency of these experiments in larger proteins.

Since much side-chain information is lost after complete deuteration of the side-chains, schemes have been developed to selectively reintroduce methyl protons into a number of aliphatic side-chains (Gardner et al., 1997; Gardner and Kay, 1998). The production of such partially reprotonated proteins is more complicated than that of partially or fully deuterated proteins. Moreover, only certain methyl groups remain protonated, making a limited set of residues available for side-chain assignment.

4D HCCH-NOESY (Fischer et al., 1996) designed to replace HCCH-TOCSY and HCCH- COSY experiments when applied to large proteins has been used to assign side-chain resonances of the gp41 ectodomain (Caffrey et al. 1997). NOE transfer between ^{13}C spins circumvents the problem of T_2 relaxation during long scalar transfer periods, and becomes advantageous for proteins with molecular weight above 20 kDa (Fischer et al., 1996). It should be noted, that despite the effectiveness of a single transfer step, HCCH-NOESY requires more experimental time due to the inherently long NOE mixing time. The experiments of this type with double selection for protonated carbon spins become less effective with increasing molecular weight and do not benefit strongly from partial deuteration.

We propose a new strategy for side-chain assignment in larger proteins. The key element in this approach is the nearly complete assignment of the side-chain ^{13}C resonances achieved with the use of ^{13}C-start and ^{13}C-observe experiments. The 2D ^{13}C-observe technology for isotopically enriched proteins was introduced by the Markley group (Oh et al., 1988; Westler et al., 1988). In the first step the conventional suite of 3D and 4D TROSY triple-resonance experiments (Salzmann et al., 1999a, b; Yang and Kay, 1999; Mulder et al., 2000) is used to assign backbone $^{1}H^{N}$, ^{15}N, $^{13}C'$, $^{13}C^{\alpha}$ and $^{13}C^{\beta}$ resonances using a uniformly deuterated and ^{13}C- and ^{15}N-labeled protein sample. In the second step the ^{13}C-start, ^{13}C-observe 2D and 3D spectroscopy is employed in order to correlate the side-chain ^{13}C chemical shifts and assign them to particular residues along the polypeptide backbone using the $^{13}C'$, $^{13}C^{\alpha}$ and $^{13}C^{\beta}$ residue specific assignment from the preceeding step. Then, 3D ^{13}C- and ^{15}N- resolved $\{^{1}H,^{1}H\}$-NOESY spectra are recorded with a partially deuterated protein. These spectra together with the assignment of the ^{13}C, $^{1}H^{N}$ and ^{15}N chemical shifts from the preceeding steps are used to assign ^{1}H resonances. A notable feature of the ^{13}C-observe experiments is that multiple and redundant $^{1}J_{CC}$ scalar couplings are resolved as ^{13}C multiplets in the directly acquired ^{13}C dimension. They can be used to measure an extensive set of the residual ^{13}C-^{13}C dipolar couplings when a slight spatial alignment of protein is introduced (Tjandra and Bax, 1997; Tjandra et al., 1997b). This, together with $\{^{1}H,^{1}H\}$ NOEs might enable high precision structure determination in larger proteins (Clore et al., 1999).

Here we demonstrate that with the use of the commercially available cryogenic NMR probe technology ^{13}C-start and ^{13}C-observe spectra can be obtained with sufficient sensitivity. This enables fast and reliable side-chain resonance assignment in large proteins. Gains in sensitivity are achieved by an addition of a paramagnetic relaxation enhancement agent in order to increase ^{13}C T_1 relaxation rates with little effect on ^{13}C T_2 rates in analogy to intrinsic paramagnetic enhancements previously used to obtain sensitive ^{13}C-spectra of paramagnetic proteins with slow electronic relaxation rates (Machonkin et al., 2002). An automated procedure for the assignment of side-chain ^{1}H chemical shifts using ^{13}C- and ^{15}N- resolved $\{^{1}H,^{1}H\}$-NOESY spectra is discussed.

Materials and methods

NMR spectroscopy

Uniformly ^{2}H,^{15}N,^{13}C-labeled and partially 35% deuterated, uniformly ^{15}N,^{13}C-labeled BsCM samples

in ^1H_2O:^2H_2O (97:3) solution (protein concentration 1 mM, pH = 7.5) were produced as described previously (Eletsky et al., 2001, 2002). An 0.5 M solution of Gd(DTPA-BMA) was purchased from Nycomed-Amersham and used without additional purification.

The ^{13}C-start, ^{13}C-observe experiments were performed on a BRUKER AVANCE 500 MHz spectrometer equipped with a cryogenic Z-gradient DUAL ^{13}C/^{1}H probe. The 2D CACO experiment, derived from MQ-HACACO (Pervushin and Eletsky, 2003), and 3D ^{15}N resolved {^{1}H,^{1}H}-TROSY-enhanced NOESY (Zhu et al., 1999) were recorded on a BRUKER AVANCE 600 MHz spectrometer equipped with a cryogenic Z-gradient TXI ^{15}N/^{13}C/^{1}H probe. The 3D ^{13}C resolved {^{1}H,^{1}H}-NOESY (Ikura et al., 1990) experiment was recorded on a BRUKER AVANCE 900 MHz spectrometer, equipped with a Z-gradient TXI probe. All NMR experiments were performed at 20 °C.

The effect of the gadolinium chelate on ^{13}C T_1 and T_2 relaxation times in the U-^{2}H,^{15}N,^{13}C-labeled BsCM sample was probed by adding 5 μl aliquots of 0.5 M Gd(DTPA- BMA) solution and acquiring a 2D CACO spectrum after each addition. The sample was subsequently dialysed, and the titration repeated except that 6 μl aliquots of 0.1 M Gd(DTPA- BMA) solution were added and ^{13}C T_1 and $^{13}C^{\alpha}$ T_2 relaxation times were measured in a series of 1D ^{13}C spectra. Saturation-recovery experiment was used to measure T_1 relaxation times. Saturation was achieved by applying a ^{13}C 90° pulse followed by a 1.0 ms PFG pulse and two orthogonal 0.5 ms high-power spin-lock pulses. T_2 relaxation times of the $^{13}C^{\alpha}$ spins were measured in a spin-echo experiment employing a 1.6 ms refocusing BURP pulse to decouple $^{13}C^{\alpha}$ spins from $^{13}C'$ and $^{13}C^{\beta}$ spins of residues other than serine and threonine. SEDUCE composite pulse decoupling of deuterium spins with $\gamma B_2 = 0.7$ kHz was applied throughout the experiment. The recovery of longitudinal and transverse ^{13}C magnetization was monitored in series of eight ^{13}C-observe experiments measured in 1D mode. Each of these series were recorded for 9 h with 1024 scans per T_1 and T_2 time increment. Titration of the U-^{2}H,^{15}N,^{13}C-labeled BsCM sample with Gd(DTPA-BMA) was stopped after an apparent decrease of the ^{13}C T_2 relaxation time was noticed. The final concentration of Gd(DTPA-BMA) comprised 6 mM, corresponding to 18 μl of 0.1 M solution added.

Paramagnetic relaxation enhancement of ^{13}C magnetization

Since the effect of a paramagnetic relaxation enhancement agent on the T_1 and T_2 relaxation times of ^{1}H spins is well established, in the following section we compare the paramagnetic relaxation enhancement rates of ^{13}C and ^{1}H spins. The theoretical analysis demonstrates that (i) the same amount of the paramagnetic agent induces similar T_1 enhancements for both ^{13}C and ^{1}H spins, (ii) the expected line broadening effect is an order of magnitude less effective for the ^{13}C spins comparing to the ^{1}H spins and (iii) the ^{13}C T_1 enhancement can be controlled by changing the concentration of the agent.

The interaction of the ^{13}C spins with small molecules bearing unpaired electronic spins can be described by a 'second-sphere interaction model' (Peters et al., 1996; Sharp et al., 2001). This model assumes that the relaxation agent and the protein molecule form a non-specific but rotationally correlated complex. Relaxation enhancement is caused by the modulation of the dipolar interaction between the electron spin and the nuclear spins due to rotational motion and depends on the correlation time τ_r, the electronic relaxation (T_{1e} and T_{2e}) and the lifetime of the complex (τ_M). The dipolar contributions $T_{1,p}$ and $T_{2,p}$ to the relaxation rates of the complexed protein are thus given by:

$$\frac{1}{T_{1,p}} = \frac{2}{15}\left(\frac{\mu_0}{4\pi}\right)^2 \frac{\gamma_I^2 (g_J \mu_B)^2 J(J+1)}{r^6} \left(\frac{3\tau_{1c}}{1+\omega_I^2\tau_{1c}^2} + \frac{7\tau_{1c}}{1+\omega_S^2\tau_{1c}^2}\right), \quad (1)$$

$$\frac{1}{T_{2,p}} = \frac{1}{15}\left(\frac{\mu_0}{4\pi}\right)^2 \frac{\gamma_I^2 (g_J \mu_B)^2 J(J+1)}{r^6} \left(4\tau_c + \frac{3\tau_{2c}}{1+\omega_I^2\tau_{2c}^2} + \frac{13\tau_{2c}}{1+\omega_S^2\tau_{2c}^2}\right), \quad (2)$$

Here $\mu_0/4\pi$ is the magnetic permeability of free space, γ_I is the gyromagnetic ratio of the nuclear spin, g_J is the Lande factor, μ_B is the Bohr magneton, J is the electron spin of the paramagnetic ion ($J = 7/2$ for Gd^{3+}), r is the distance from the nucleus to the paramagnetic center, and ω_I and ω_S are the nuclear and the electronic Larmor frequencies, respectively. The effective correlation times τ_{ic} are given by:

$$\frac{1}{\tau_{ic}} = \frac{1}{T_{ie}} + \frac{1}{\tau_M} + \frac{1}{\tau_r}, \quad \text{where } i = 1, 2. \quad (3)$$

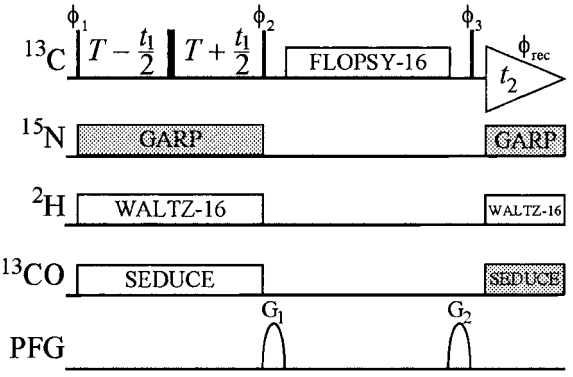

Figure 1. Experimental scheme of the 2D ^{13}C-start and ^{13}C-observe constant-time {^{13}C,^{13}C}-TOCSY experiment. The non-constant time variant is obtained by replacing T$-t_1/2$ by $t_1/2$ and T$+t_1/2$ by $t_1/2$. The radio-frequency pulses on ^{13}C, ^{15}N, ^{2}H, and ^{13}C′ are applied at 40, 118, 3.2 and 174 ppm, respectively. Narrow and wide black bars indicate non-selective 90° and 180° pulses, respectively. The line marked PFG indicates the duration and strength of pulsed magnetic field gradients applied along the z-axis: G_1: 800 μs, 80 G/cm and G_2: 800 μs, 70 G/cm. The constant-time delay $T = 1/(2\,{}^1J_{CC})$ is set to 13.5 ms. The phases are defined as follows: $\phi_1 = \{x, -x\}$, $\phi_2 = \{x\}$, $\phi_3 = \{y\}$ and $\phi_{rec} = \{x, -x\}$. Quadrature detection in the $^{13}C(t_1)$ dimension is achieved by the States-TPPI method (Marion et al., 1989) applied to the phase ϕ_1. ^{2}H-decoupling during t_1 and t_2 is achieved with WALTZ-16 (Shaka et al., 1983) at the field strength of $\gamma B_2 =$ 2.5 kHz. ^{13}C′-decoupling during t_1 is achieved with SEDUCE (Shaka et al., 1983) at a field strength of $\gamma B_2 = 0.5$ kHz. Although important for optimization of the sensitivity of the experiment, the shaded composite pulse decoupling elements were not performed due to hardware limitations.

In experiments with Gd(DTPA-BMA) and ubiquitin, τ_M was found to be 0.6 ns (Pintacuda and Otting, 2002). This value is determined by translational diffusion of the interacting species, and since Gd(DTPA-BMA) is much smaller than protein molecules (3.5 Å vs. 14 Å for ubiquitin or 23 Å for BsCM) it can be viewed as a property of Gd(DTPA-BMA) alone. The electronic relaxation times T_{1e} and T_{2e} were estimated to be 80 ns (Powell et al., 1996) and 4 ns (Peters et al., 1996), respectively, thus, they are much longer than τ_M. The rotational correlation time τ_r of ubiquitin is 4 ns (Pintacuda and Otting, 2002). Therefore, for proteins of the size of ubiquitin and larger, $\tau_r \gg \tau_M$ and the correlation times τ_{ic} are approximately constant and equal to τ_M. The same holds for BsCM, whose τ_r is estimated to be 20 ns. With $\tau_c = 0.6$ ns the terms containing the electron Larmor frequencies in Equations 1 and 2 can be safely neglected.

A numerical evaluation of Equations 1 and 2 for ^{13}C spins in BsCM at 600 MHz polarizing magnetic field strength yields $\omega_I^2\tau_c^2 = 0.3$ and $1/T_{1,p}(^1\text{H}) = 3.4/T_{1,p}(^{13}\text{C})$, $1/T_{2,p}(^1\text{H}) = 11.3/T_{2,p}(^{13}\text{C})$ and $1/T_{1,p}(^{13}\text{C}) = 0.7/T_{2,p}(^{13}\text{C})$. The T_1 and T_2 relaxation times of the ^{13}C spins in proteins are markedly different, the former having values on the order of seconds, and the latter on the order of tens of milliseconds. The fact, that longitudinal and transverse relaxation enhancements in a complex with a paramagnetic agent are comparable, indicates a possibility of reducing ^{13}C T_1 with practically no effect on ^{13}C T_2.

In order to estimate how the relaxation enhancement of the protein ^{13}C spins will be manifested in NMR experiments, the extreme narrowing approximation could be invoked. The condition for that is given by Equation 4 (Peters et al., 1996):

$$\left|\frac{1}{\tau_M}+\frac{1}{\tau_f}\right| \gg \Delta\omega_{Mf}, \quad \left|\frac{1}{T_{i,M}}-\frac{1}{T_{i,f}}\right| \quad i = 1, 2, \qquad (4)$$

where τ_f is the residence time of free protein, $\Delta\omega_{Mf} = |\omega_M - \omega_f|$ is the frequency shift, $T_{i,M}$ and $T_{i,f}$ are the relaxation times of bound and free protein molecules, respectively. This approximation corresponds to the case, when a single line per spin with averaged relaxation properties is observed for both free and complexed states. The observed chemical shift is:

$$\omega_{obs} = \omega_M f_M + \omega_f f_f, \qquad (5)$$

and the relaxation rates are:

$$\frac{1}{T_{1,obs}} = \frac{f_M}{T_{1,M}} + \frac{f_f}{T_{1,f}}, \qquad (6)$$

$$\frac{1}{T_{2,obs}} = \frac{f_M}{T_{2,M}} + \frac{f_f}{T_{2,f}} + f_M f_f \Delta\omega_{Mf}^2 \left(\frac{1}{\tau_M}+\frac{1}{\tau_f}\right)^{-1}, \qquad (7)$$

where f_M and f_f are the fractions of bound and free protein, respectively. Taking into account that $f_M + f_f = 1$, and assuming that paramagnetic relaxation is governed only by dipolar terms,

$$\frac{1}{T_{i,M}} = \frac{1}{T_{i,f}} + \frac{1}{T_{i,p}}, \quad i = 1, 2, \qquad (8)$$

we can rewrite Equations 6 and 7 as

$$\frac{1}{T_{1,obs}} = \frac{f_M}{T_{1,M}} + \frac{1}{T_{1,f}}, \qquad (9)$$

$$\frac{1}{T_{2,\mathrm{obs}}} = \frac{f_M}{T_{2,p}} + \frac{1}{T_{2,f}} + f_M f_f \Delta\omega_{Mf}^2 \left(\frac{1}{\tau_M} + \frac{1}{\tau_f}\right)^{-1}. \quad (10)$$

If there is no frequency shift ($\Delta\omega_{Mf} = 0$), then both relaxation enhancements are equal to the dipolar paramagnetic terms, scaled by the factor f_M. The fraction of the bound protein molecules f_M is, in turn, directly proportional to the concentration of the paramagnetic chelate. The resulting relaxation rates can thus be controlled by varying the concentration of the paramagnetic agent.

Results and discussion

The atom-specific assignment of the ^{1}H, ^{15}N and ^{13}C resonances in BsCM, which is a prerequisite for the structure determination, was done in three consecutive steps. In the first step the complete residue-specific assignment of backbone $^1H^N$, ^{15}N, $^{13}C^\alpha$ and $^{13}C'$ and $^{13}C^\beta$ resonances was done. The standard set of 3D and 4D TROSY type of triple resonance experiments (Salzmann et al., 1999a, b; Yang and Kay, 1999; Mulder et al., 2000) was applied to the uniformly deuterated and ^{13}C,^{15}N-labeled BsCM (Eletsky et al., 2001). In addition a partially deuterated and ^{13}C,^{15}N-labeled BsCM sample was used to assign $^1H^\alpha$ resonances using the ^{13}C-detected multiple-quantum HACACO experiment (Pervushin and Eletsky, 2003). In the subsequent step 90% of the ^{13}C resonances in long side-chains were assigned by means of the ^{13}C-start, ^{13}C-observe experiments. In the last step ^{15}N-resolved and ^{13}C-resolved NOESY experiments were used to assign ^{1}H side-chain resonances.

Assignment of the side-chain aliphatic ^{13}C resonances

Two ^{13}C-start, ^{13}C-observe spectra, a 2D ^{13}C TOCSY and a 2D ^{13}C constant-time TOCSY of Figure 1 were used to assign aliphatic side-chain ^{13}C resonances to particular carbon atoms. Figure 2 shows a combined representation of the ^{13}C ct-TOCSY and ^{13}C TOCSY spectra placed above and below the diagonal, respectively. The apparent complexity of these spectra is effectively offset by narrow linewidths in the ω_2 dimension. While the ^{13}C constant-time TOCSY experiment is estimated to be two times less sensitive than the conventional ^{13}C TOCSY, it offers a much better resolution in the indirect dimension. In addition, it allows ^{13}C spins with different numbers n of directly attached carbons to be distinguished based on the sign of the cross-peaks according to $\cos^n(2\pi^1 J_{CC}T)$, where 2T is the duration of the ^{13}C constant time period in Figure 1. The cross-peaks from $^{13}C^\alpha$ spins in the ω_1 dimension of the constant-time spectrum are weakened by the scalar coupling to backbone ^{15}N spins which could not be decoupled with the available instrumentation.

The assignment proceeded as follows. First, covalently connected spin systems of certain amino acid types were extracted in analogy to homonuclear proton spectroscopy (Wüthrich, 1986). Based on their distinct chemical shifts the spin systems of Ser, Thr, Pro and all methyl group-containing amino acids were identified in the 2D ^{13}C TOCSY spectrum. Overlapping side-chain resonances of Val and Leu were sufficiently resolved in the 2D ^{13}C constant-time TOCSY experiment. The higher resolution was indispensable for assignment of arginine and lysine side-chains as demonstrated in Figure 3 for Lys25. Identification of the spin systems containing methyl groups was facilitated by the large spectral dispersion of ^{13}C methyl resonances, as shown in Figure 4. Although the multiplet structure observed in the ω_2 dimension for practically all cross-peaks (Figure 4) contributed to spectral complexity, it helped with the spin system type identification.

Spin systems were then assigned to particular amino acids using the sequential assignment of $^{13}C^\alpha$ and $^{13}C^\beta$ chemical shifts obtained from the TROSY-HNCA and TROSY- HNCACB experiments. In many cases, $^{13}C^\alpha$ chemical shifts alone sufficed to assign a spin system to a particular residue. Because backbone and side-chain ^{13}C chemical shifts are measured using the same uniformly ^{2}H,^{13}C,^{15}N-labeled sample, no correction for the ^{1}H/^{2}H isotope effect is needed. This, in turn, increases the resulting precision of ^{13}C chemical shift measurement and reduces tolerances for matching chemical shifts in the different spectra. Table 2 summarizes the assignment of aliphatic spin systems obtained from the two ^{13}C TOCSY spectra. All ^{13}C resonances in long aliphatic side-chains have been assigned with the exception of leucine residues, where the assignment is impeded by the general problem of overlapping $^{13}C^\gamma$ and $^{13}C^\delta$ chemical shifts. At present, side-chain carbonyl, carboxyl and aromatic ^{13}C resonances have not been assigned. For this purpose extensions of the reported experimental schemes are required. These are currently under development.

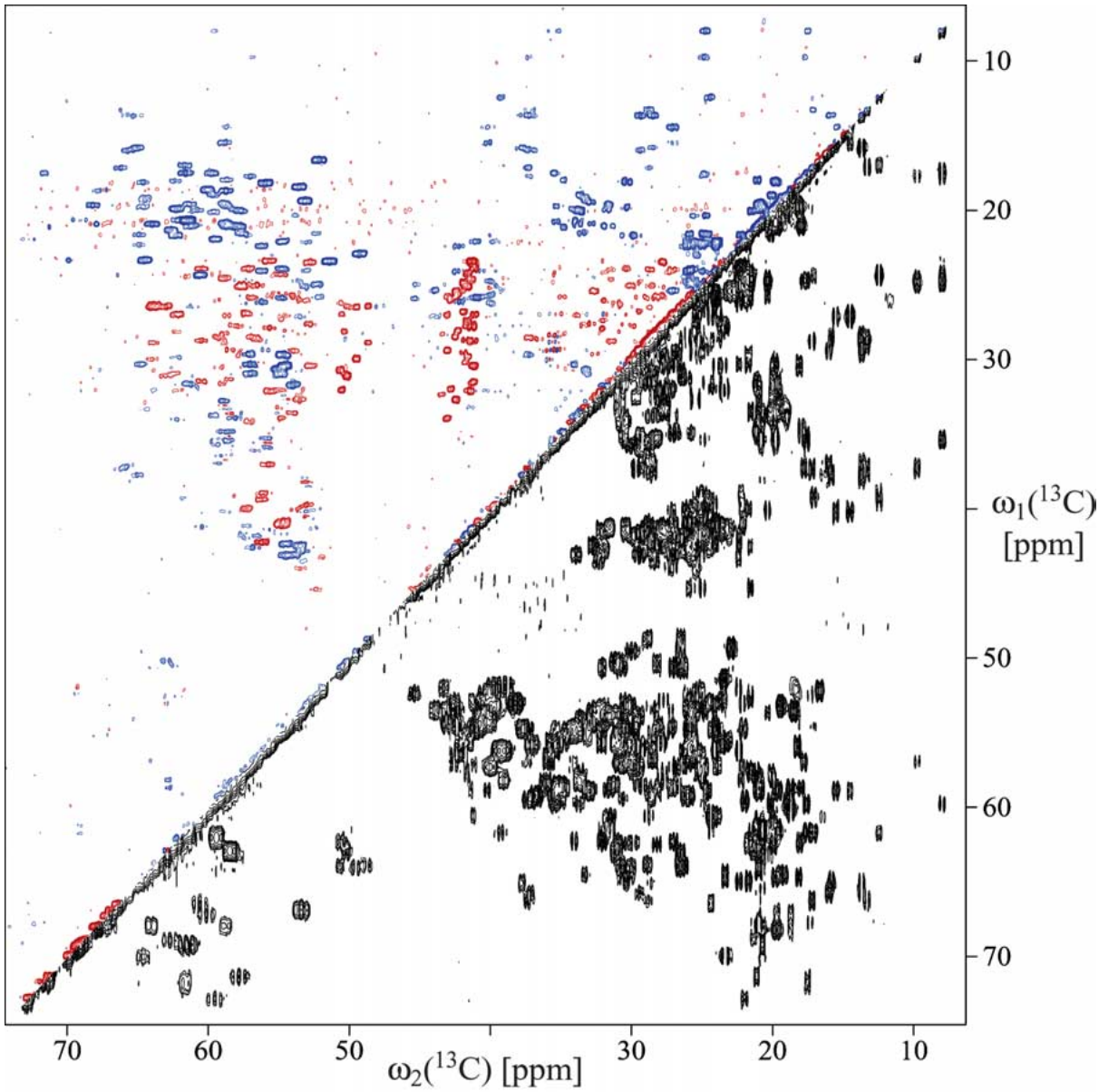

Figure 2. 2D ^{13}C constant-time TOCSY spectrum (above diagonal) and 2D ^{13}C TOCSY spectrum (below diagonal) of the 44 kDa uniformly ^{2}H,^{13}C,^{15}N-labeled BsCM measured with the experimental scheme of Figure 1. In both experiments the ^{13}C carrier position is set to 40 ppm, spectral width is 10 kHz in each dimension and isotropic mixing is achieved with the 16 ms FLOPSY-16 sequence (Kadkhodaie et al., 1991) with $\gamma B_1 = 8.2$ kHz. The sample of U-^{2}H,^{13}C,^{15}N-labeled BsCM used to record the ^{13}C constant-time TOCSY contained 6 mM Gd(DTPA-BMA). $1024(t_2) \times 520(t_1)$ complex points were recorded with 200 scans per increment, $2T = 27$ ms and 3.0 s recycle delay resulting in 96 h of measuring time. The same protein sample, but without Gd(DTPA-BMA) was used to record the 2D ^{13}C TOCSY spectrum. $1024(t_2) \times 90(t_1)$ complex points were recorded with 160 scans per increment, $t_{1,\max} = 9$ ms and 4.5 s recycle delay, resulting in 36 h of measuring time. In this case the SEDUCE sequence of Figure 1 was replaced by a single 100 μs gaussian $^{13}C'$ 180° pulse applied in the middle of the t_1 period in order to refocus evolution due to scalar couplings to carbonyl spins. Positive and negative cross-peaks are colored blue and red, respectively.

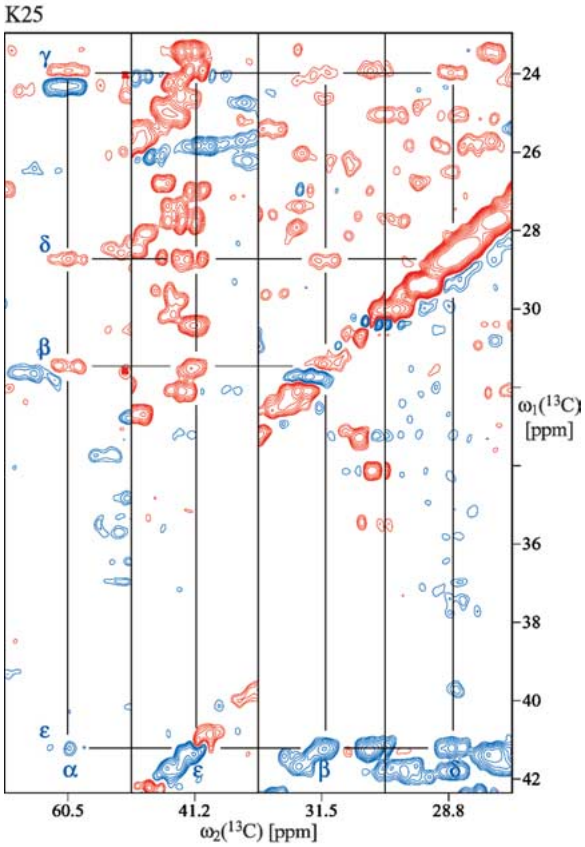

Figure 3. Four 2D regions of the constant-time ^{13}C TOCSY spectrum of Figure 2 aligned along the $\omega_1(^{13}C)$ dimension illustrating the assignment of the ^{13}C side-chain chemical shifts of Lys25. The narrow $^{13}C^{\varepsilon}$ doublet of Lys25 at 41.2 ppm along ω_2 is used as a starting point to trace the connectivities within the side-chain ^{13}C spin system shown by thin lines. The spin system is then assigned residue-specifically by matching the observed $^{13}C^{\alpha}$ and $^{13}C^{\beta}$ chemical shifts with those identified during the backbone resonance assignment process. The relative sign of the cross-peaks is defined by the number of ^{13}C spins covalently attached to the ^{13}C spin whose chemical shift is detected along the ω_1 dimension. This information together with the multiplet structure of cross-peaks observed along the ω_2 dimension allows unambiguous assignment of ^{13}C spins in the side-chain.

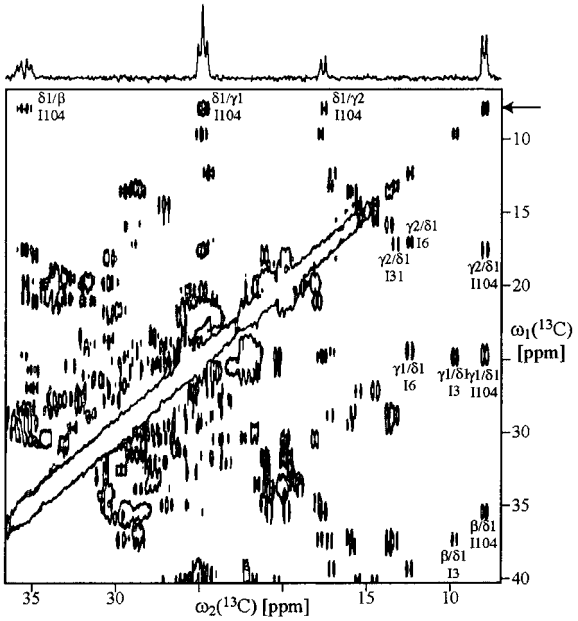

Figure 4. An expansion of the 2D ^{13}C TOCSY spectrum of U-^{2}H,^{13}C,^{15}N-labeled BsCM illustrating the resolved multiplet structure observed along the directly detected ^{13}C dimension. Individual cross-peaks are labeled according to their assignment along the ω_1 and ω_2 dimensions, respectively. A 1D ^{13}C slice at the top is taken along ω_2 at the chemical shift of $^{13}C^{\delta 1}$ of Ile104 as indicated by an arrow.

To provide a better match between backbone and side-chain ^{13}C chemical shifts, the $^{13}C'$ chemical shifts can also be used. More complicated magnetization transfer pathways involving $^{13}C'$ spins, can be considered. This is warranted by the sufficiently long transverse relaxation times of ^{13}C spins in deuterated proteins when NMR experiments are conducted at low polarizing magnetic fields in the range of 500 to 600 MHz. Another improvement of the sensitivity and resolution of the spectra in Figure 2 is expected from the use of ^{15}N and $^{13}C'$ decoupling during signal acquisition and ^{15}N decoupling during the constant-time period 2T (Figure 1). These tasks are limited at present by the available hardware.

Since the ^{13}C-start, ^{13}C-observe experiments are central to the proposed strategy, it is instructive to analyze factors contributing to the resulting sensitivity of the ^{13}C spectra of larger proteins.

^{13}C T_1 and T_2 relaxation in uniformly perdeuterated BsCM

The applicability of the NMR experiments utilizing ^{13}C-detection in studies of large biomolecules is limited by several factors, such as the expected sensitivity, which is $(\gamma_H/\gamma_C)^{3/2} \sim 8$ times lower in ^{13}C spectra compared to ^{1}H spectra (Reynolds and Enriquez, 2002), long ^{13}C T_1 relaxation times and the very fast ^{13}C transverse relaxation (Grzesiek et al., 1993). The first of these three problems can be alleviated to a significant extent by the use of cryogenic probes optimized for ^{13}C-detection. In uniformly deuterated proteins both longitudinal and transverse relaxation rates of the aliphatic ^{13}C spins are significantly decreased when covalently attached ^{1}H spins are replaced with

^{2}H. Perdeuteration leads to prolonged ^{13}C T_1 relaxation times in the range of 5–12 s (Venters et al., 1996). However, the sensitivity losses associated with the long longitudinal relaxation time T_1 of carbon spins can be reduced by adding paramagnetic compounds into the protein solution. Gadolinuim chelates are effective relaxation enhancers due to their high electronic spin state ($J = 7/2$) and long electronic longitudinal relaxation time. Several such compounds, for instance, Gd(DTPA-BMA), are commercially available as contrast agents for magnetic resonance imaging. An increase of $1/T_1$ of ^{1}H spins in the range of 2-3 s^{-1} was observed for ubiquitin in a 5 mM solution of Gd(DTPA-BMA) (Pintacuda and Otting 2002) without significant perturbations of the isotropic ^{1}H chemical shifts in the protein. A comparable longitudinal relaxation enhancement of ^{13}C spins can be achieved using slightly higher concentrations of Gd(DTPA-BMA) (see Material and methods). Although the ^{13}C T_1 enhancement decreases with the distance from the protein surface, longitudinal relaxation of many ^{13}C spins can be significantly enhanced.

To demonstrate this effect a series of 2D CACO spectra of U-^{2}H,^{13}C,^{15}N-labeled BsCM was acquired with increasing concentrations of Gd(DTPA-BMA). Figure 5 illustrates that there is an improvement in intensity of many cross-peaks with corresponding residues located up to 15 Å from the solvent-accessible surface of BsCM. The S/N enhancement reaches its optimum at around 10 mM for the concentration of Gd(DTPA-BMA), decreasing at larger concentrations due to ^{13}C line broadening.

The longitudinal and transverse relaxation times of all types of ^{13}C spins were measured in a series of 1D ^{13}C-detected experiments with and without gadolinium chelate. The values are reported in Table 1. Reductions in T_1 by factors 2–3 were observed for all types of ^{13}C spins. For individually resolved ^{13}C resonances (e.g., Ala112 $^{13}C^{\beta}$, Ile32 $^{13}C^{\gamma 2}$, Ile89 $^{13}C^{\gamma 2}$, Ile89 $^{13}C^{\delta 1}$, Ile6 $^{13}C^{\delta 1}$, Ile104 $^{13}C^{\delta 1}$) the T_1 reductions can be correlated with the position of the corresponding ^{13}C spins in the protein 3D structure (Chook et al., 1994). Large $1/T_{1,p}$ factors on the order of 0.2–0.3 s^{-1} were observed for Ala112 $^{13}C^{\beta}$ and Ile32 $^{13}C^{\gamma 2}$ which are located only a few angstroms from the solvent-accessible protein surface. On the other hand, the longitudinal relaxation rates of the relatively buried $^{13}C^{\delta 1}$ spins of Ile6 and Ile89 were increased by only 0.1 s^{-1}. The largest enhancements, on the order of 1.25–3 s^{-1}, were observed for backbone $^{13}C'$ spins and the $^{13}C^{\zeta}$ spins of arginines. On average, paramagnetic T_2 relaxation enhancements of 3.0 s^{-1} were also observed, the values being 1.5 times larger than can be estimated from T_1 relaxation enhancement values using Equations 1 and 2. Small chemical shift perturbations not exceeding 0.1 ppm have been observed for some resonances. In general, the data is in qualitative agreement with the theoretical predictions indicating that ^{13}C T_1 relaxation times can be reduced without significantly affecting ^{13}C T_2 relaxation times.

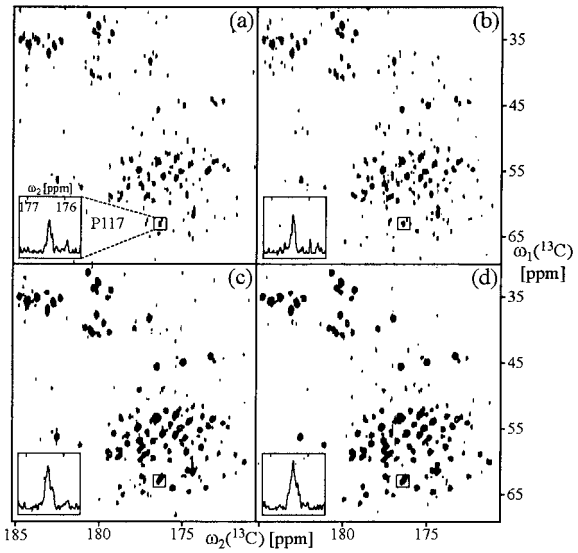

Figure 5. Sensitivity enhancement of ^{13}C spectra induced by the paramagnetic compound Gd(DTPA-BMA). A region of the ^{13}C-start, ^{13}C-observe 2D CACO spectrum is shown containing cross-peaks involving chemical shift correlations from side-chain $^{13}C/^{13}C'$ and backbone $^{13}C^{\alpha}/^{13}C'$ atoms measured with the uniformly ^{2}H,^{13}C,^{15}N-labeled BsCM in the presence of (a) 0 mM, (b) 10 mM, (c) 20 mM and (d) 30 mM Gd(DTPA-BMA). The carrier positions and spectral widths are 177 ppm and 3.0 kHz in $\omega_2(^{13}CO)$, and 42 ppm and 8.3 kHz in $\omega_1(^{13}C)$, respectively. $512(t_2) \times 72(t_1)$ complex points with 256 scans per increment and a fixed recycle delay of 0.8 s were recorded resulting in 15 h of measuring time per spectrum. The 1D $^{13}C'$ slices along the ω_2 dimension taken at the $^{13}C^{\alpha}$ chemical shift of Pro117 are shown in the corresponding insets.

Assignment of the side-chain ^{1}H resonances

Here we propose an algorithm which uses the complete backbone and side-chain ^{13}C assignment as a starting point for analysis of ^{13}C- and ^{15}N-resolved NOESY spectra with the goal of identifying ^{1}H chemical shifts of the spin system. It relies on correlations between NOESY cross-peaks occurring in different planes of the 3D data sets and is therefore effective for aliphatic side-chain fragments such as Ala, Thr,

Table 1. Characteristic ^{13}C T_1 and T_2 relaxation times measured in U-^{2}H,^{13}C,^{15}N-labeled BsCM in the presence of 0 and 6 mM of Gd(DTPA-BMA)

Spin[a]	ω [ppm][b]	T_1 [s] 0 mM	T_1, [s] 6 mM	T_2, [ms] 0 mM	T_2, [ms] 6 mM
13C′	180.37	3.29 ± 0.09	0.57 ± 0.05		
	176.76	4.20 ± 0.11	1.10 ± 0.07		
	174.14	3.93 ± 0.10	1.70 ± 0.11		
13C$^{\zeta}$ (R)	160.40	2.90 ± 0.25	1.85 ± 0.11		
	159.64	1.51 ± 0.03	0.22 ± 0.01		
13C^{Arom}	133.07	2.74 ± 0.17	0.83 ± 0.06		
	130.31	3.19 ± 0.29	1.29 ± 0.10		
	119.97	3.01 ± 0.15	0.77 ± 0.06		
13C$^{\alpha}$	55.92	3.48 ± 0.13	1.07 ± 0.06	46 ± 3	40 ± 4
	53.50	4.46 ± 0.16	1.74 ± 0.08	33 ± 2	26 ± 2
	52.11	5.59 ± 0.57	1.72 ± 0.17	31 ± 4	24 ± 4
13C^{Aliph}	41.55	2.35 ± 0.04	0.35 ± 0.01		
	35.56	2.25 ± 0.11	0.78 ± 0.06		
	29.42	2.43 ± 0.09	0.92 ± 0.05		
13C^{Methyl}	22.27	4.2 ± 0.1	1.1 ± 0.1		
	18.38	4.6 ± 0.3	1.3 ± 0.1		
	16.90	8.7 ± 0.6	2.9 ± 0.2		
Ala112 β	16.54	4.5 ± 0.6	1.9 ± 0.4		
Met ε	16.32	9.0 ± 1.1	0.8 ± 0.1		
Met ε	16.23	10.5 ± 1.2	3.1 ± 0.3		
Ile32 γ2	15.99	4.6 ± 0.4	1.9 ± 0.3		
Met ε	15.88	3.4 ± 0.4	2.9 ± 0.5		
Ile89 γ2	15.4	5.1 ± 0.9	3.3 ± 1.0		
Met ε	15.02	5.9 ± 1.1	4.7 ± 1.3		
Ile89 δ1	14.66	9.4 ± 1.6	3.7 ± 1.3		
Ile6 δ1	12.33	6.0 ± 1.3	4.0 ± 1.6		
Ile104 δ1	7.87	7.8 ± 0.6	3.8 ± 1.7		

[a]The assignment of the corresponding resonance in the 1D ^{13}C spectrum to a certain atom type was based on the characteristic chemical shifts. Individually resolved resonances were assigned residue-specifically.
[b]For the values listed for $^{13}C'$, $^{13}C^{\zeta}$ (R), $^{13}C^{Arom}$, $^{13}C^{\alpha}$, $^{13}C^{Aliph}$, several overlapping resonances were used to determine the ^{13}C T_1 and T_2 relaxation times.

Pro, Ile, Val, Leu, Arg and Lys. The assignment of the ^{1}H spins requires complete or partial protonation of side-chains. Following the standard approach of the HCCH-TOCSY and HCCH-COSY experiments (Cavanagh et al., 1996) only a few of the side-chain ^{1}H resonances were obtained for the partially 35% deuterated and uniformly ^{15}N,^{13}C-labeled 44 kDa BsCM due to the fast ^{13}C transverse relaxation in ^{13}C-^{1}H moieties. On the other hand, rather sensitive 3D ^{13}C-resolved and ^{15}N-resolved {^{1}H,^{1}H} NOESY spectra with high sensitivity and resolution were obtained with the same sample using NMR spectrometers operating at 900 and 600 MHz, respectively (Figure 6). We illustrate the method in detail with the assignment of the side-chain ^{1}H resonances of Ile104, where all backbone and ^{13}C side-chain resonances were assigned as described previously (see Figure 4).

First, 2D {^{1}H,^{1}H} NOESY planes are extracted at the positions of the ^{15}N and ^{13}C chemical shifts of Ile104 corrected for the $^{1}H/^{2}H$ isotope effect (Venters et al. 1996) as shown in Figure 6. Each extracted NOESY plane is analyzed for chemical shift values along $\omega_3(^{1}H)$ which exhibit numerous aligned cross-peaks along $\omega_2(^{1}H)$. We refer to a group of such aligned peaks as a NOESY tower. Each extracted plane contains a limited number of NOESY towers at different $\omega_3(^{1}H)$ positions (usually 3–15), which must include the ^{1}H chemical shift of the ^{1}H spin covalently

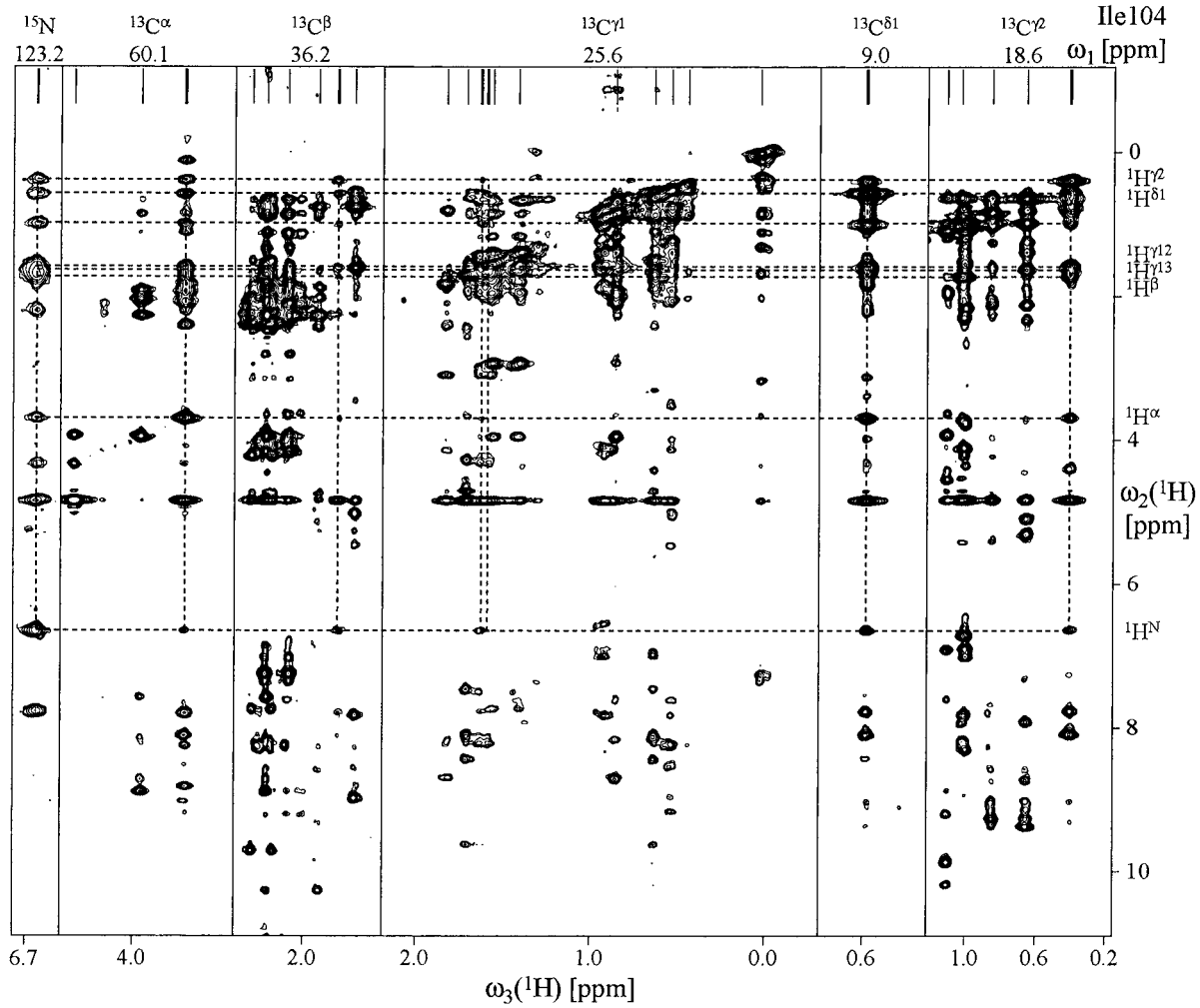

Figure 6. An assignment strategy for the ^{1}H side-chain chemical shifts in protonated or partially deuterated proteins when the complete assignments for ^{15}N and ^{13}C chemical shifts are available, illustrated with the side-chain of Ile104 from BsCM. 2D {^{1}H,^{1}H} NOESY planes are taken from 3D ^{15}N-resolved and ^{13}C-resolved NOESY spectra of partially (35%) deuterated, ^{13}C,^{15}N-labeled BsCM at the positions of ^{15}N, $^{13}C^{\alpha}$, $^{13}C^{\beta}$, $^{13}C^{\gamma 1}$, $^{13}C^{\delta 2}$ and $^{13}C^{\gamma 2}$ chemical shifts of Ile104 corrected for the ^{2}H/^{1}H isotope effect (Venters et al., 1996). Only the spectral region centered around the $^{1}H^{N}$ resonance of Ile104 is shown for the ^{15}N-resolved NOESY. All cross-peaks found in the {^{1}H,^{1}H} planes at the positions of the ^{13}C chemical shifts of Ile104 in the ^{13}C-resolved NOESY spectrum are shown. A group of such aligned peaks is referred as a NOESY tower. Each extracted plane contains a limited number of NOESY towers at different ω_3(^{1}H) positions. Thin lines on top edge of the spectrum mark proton signals in the ω_3(^{1}H) dimension, while thick lines indicate the ^{1}H assignment with the highest score function Σ. Dashed lines drawn at the ^{1}H resonance positions of Ile104 visualize the NOE connectivities within the ^{1}H spin system.

attached to the heterospin defining the plane. For example, 6, 11, 1 and 5 distinct ^{1}H resonances were found along the ω_3(^{1}H) dimension in the 2D {^{1}H,^{1}H} NOESY planes taken at the positions of the $^{13}C^{\beta}$, $^{13}C^{\gamma 1}$, $^{13}C^{\delta 1}$ and $^{13}C^{\gamma 2}$ chemical shifts of Ile104, respectively. We assume that the $^{1}H^{N}$ and $^{1}H^{\alpha}$ chemical shifts of Ile104 are known from the TROSY-HNCA (Eletsky et al., 2001) and MQ-HACACO (Pervushin and Eletsky, 2003) experiments. All combinatorial variants of the side-chain ^{1}H assignments are then constructed ($6 \times 11 \times 1 \times 5 = 330$ for Ile104) and assessed based on a score function Σ_i, where a high Σ_i value indicates that the assignment variant i is plausible. The score Σ_i is calculated as follows: Σ_i is set to $4^{*}n$ if n pairs of the diagonal-peaks defined by the ω_3 chemical shifts are connected by two NOESY cross-peaks. In Figure 6 these cross-peaks are found, for example, at the intersections of the dashed lines. The score is incremented by 1^{*}m if m diagonal-peaks are connected by one NOESY cross-peak. Figure 7

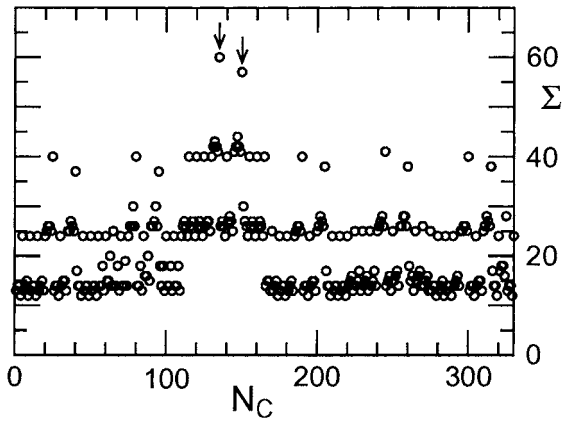

Figure 7. Results of the automatic search for the ^{1}H resonances which can be assigned to the spin system of Ile104 based on the scoring function Σ. A variant of assignment, N_c, is systematically constructed by assigning $^1H^{\beta}$, $^1H^{\gamma 1}$, $^1H^{\delta 2}$ and $^1H^{\gamma 2}$ to the chemical shifts of an arbitrary *i*th, *j*th, *k*th and *l*th ^{1}H resonances found along the ω_3 dimension in the $\{^1H,^1H\}$ planes taken at the $^{13}C^{\beta}$, $^{13}C^{\gamma 1}$, $^{13}C^{\delta 2}$ and $^{13}C^{\gamma 2}$ positions (see Figure 6), respectively. For each variant i the score function Σ_i is calculated. Vertical arrows indicate two variants of assignment with the highest scores of 60 and 57. The variant with $\Sigma_i = 60$ correspond to the ^{1}H assignment found manually and shown in Figure 6. The two variants differ in their assignment to the $^1H^{\gamma 12}$ and $^1H^{\gamma 13}$ spins and are equally valid since stereospecific assignment is not possible at the current stage.

displays the values of Σ_i ($i = 1 \ldots 330$) obtained after exhaustive search of all 330 assignment variants of the ^{1}H resonances of Ile104. Vertical arrows indicate the two assignment variants of with the highest scores of 60 and 57. Two variants in the $^{13}C^{\gamma 1}$ plane differ in the $^1H^{\gamma 12}$ and $^1H^{\gamma 13}$ assignment, since the algorithm does not distinguish the stereospecific assignment. This process is repeated for other residues. This results in a manageable number of global variants of ^{1}H assignment on the order of several hundreds, which can be used as starting points for input into NMR structure calculation programs (Guntert et al., 1997; Mumenthaler et al., 1997). With the refinement of the proposed algorithm we expect to reduce the number of variants of the ^{1}H assignment to the level where a convergence of structure calculations can be used as a criterion for the acceptance of the assignment.

Perspectives for structure determination of larger proteins

Structure determination is based on the recovery of interproton distance restraints from ^{13}C-resolved and ^{15}N-resolved $\{^1H,^1H\}$-NOESY spectra followed by structure calculation by minimizing target function including distance restraints (e.g., DYANA/CANDID programs (Guntert et al., 1997; Mumenthaler et al., 1997)). The structure calculations can be repeated in the case if several variants of the proton chemical shifts are available after ^{13}C and ^{1}H side-chain assignment using ^{13}C-start, ^{13}C-observe and NOESY experiments.

Table 2. An overview of the completeness of ^{13}C side-chain assignments in uniformly ^{2}H,^{13}C,^{15}N-labeled BsCM

Residue[a]	Assigned	Total
Thr	12	12
Ala	6	6
Ile	7	7
Leu	4	13
Val	14	14
Pro	6	6
Arg	7	7
Ser	3	3
Lys	9	9

[a]For all other residues only the $^{13}C^{\alpha}$ and $^{13}C^{\beta}$ resonances were currently assigned.

In addition, in partially aligned samples, the very narrow ^{13}C lines detected in the absence of ^{1}H spins enable measurements of a large number of residual dipolar couplings for almost every covalently linked ^{13}C-^{13}C spin pair even in large proteins, provided that the necessary degree of anisotropy is introduced to the brownian rotational diffusion of proteins (Tjandra and Bax, 1997). New techniques are being developed for membrane proteins such as the use of the mechanically compressed polyacrylamide gels containing some amount of detergent to solubilize membrane proteins (Chou et al., 2001). The technique was first proposed and successfully applied for soluble proteins (Sass et al., 2000; Tycko et al., 2000).

Thus, the efficient and sensitive detection of the ^{13}C resonances as described here represents a promising avenue for the 3D structure determination of larger biological systems. We obtained ^{1}H and ^{13}C chemical shift assignment of side-chains by using two important innovations in the NMR spectroscopy: (i) introduction of the cryogenic probe technology for sensitive detection of ^{13}C spins, (ii) the use of paramagnetic relaxation enhancement agents to handle slow longitudinal relaxation of ^{13}C spins in large proteins. The 2D ^{13}C TOCSY experiments performed even at 500 MHz polarizing magnetic field strength yield

spectra of manageable complexity to allow side-chain assignment in a 44 kDa trimeric protein. The use of higher magnetic fields and an extension of these experiments to three dimensions by including $^{13}C'$ spins would make this approach applicable to even larger systems. Other potential developments include J-resolved ^{13}C-^{13}C TOCSY and COSY, ^{13}C-observe version of $\{^{13}C,^{13}C\}$ NOESY (Fischer et al., 1996), experiments designed for the assignment of side-chain aromatic carbon spins and experiments involving ^{13}C to ^{13}C polarization transfer using planar hamiltonians and spin waves (Madi et al., 1997).

The availability of the nearly complete ^{13}C assignment together with multiple and redundant ^{13}C-^{13}C RDCs in the side-chains opens a novel avenue in the field of the computer based structure reconstruction utilizing NMR data. We expect that the ideas related to ^{1}H assignment reported in the current paper for structure reconstruction methods without explicit side-chain ^{1}H assignment will be developed further. The combination of this new line of NMR experiments and computational approaches can bring into reality detailed structure calculations of proteins in the range of 100 kDa.

Acknowledgements

Financial support was obtained from an ETH Zürich internal grant to K.P. We thank Silantes AG for providing us with the ^{15}N-, ^{13}C- and $^{2}H(<35\%)$-labeled bacterial growth medium for the BsCM preparation. We thank Prof Donald Hilvert and Alexander Kienhöfer, ETH Zürich, for the preparation of the NMR samples of BsCM. We thank Dr Fred Damberger for careful reading of the manuscript.

References

Arora, A. and Tamm, L.K. (2001) *Curr. Opin. Struct. Biol.*, **11**, 540–547.

Bax, A. (1994) *Curr. Opin. Struct. Biol.*, **4**, 738–744.

Browne, D.T., Kenyon, G.L., Packer, E.L., Sternlic, H and Wilson, D.M. (1973) *J. Am. Chem. Soc.*, **95**, 1316–1323.

Caffrey, M., Cai, M.L., Kaufman, J., Stahl, S.J., Wingfield, P.T., Gronenborn, A.M. and Clore, G.M. (1997) *J. Mol. Biol.*, **271**, 819–826.

Cavanagh, J., Fairbrother, W.J., Palmer, A.G. and Skelton, N.J. (1996) *Protein NMR Spectroscopy: Principles and Practice*, Academic Press, New York, NY.

Chook, Y.M., Gray, J.V., Ke, H.M. and Lipscomb, W.N. (1994) *J. Mol. Biol.*, **240**, 476–500.

Chou, J.J., Gaemers, S., Howder, B., Louis, J.M. and Bax, A. (2001) *J. Biomol. NMR*, **21**, 377–382.

Choy, W.Y., Tollinger, M., Mueller, G.A. and Kay, L.E. (2001) *J. Biomol. NMR*, **21**, 31–40.

Clore, G.M. and Gronenborn, A.M. (1991) *Science*, **252**, 1390–1399.

Clore, G.M. and Gronenborn, A.M. (1997) *Nat. Struct. Biol.*, **4** (Suppl.), 849–853.

Clore, G.M. and Gronenborn, A.M. (1998) *Curr. Opin. Chem. Biol.*, **2**, 564–570.

Clore, G.M. and Schwieters, C.D. (2002) *Curr. Opin. Struct. Biol.*, **12**, 146–153.

Clore, G.M., Starich, M.R., Bewley, C.A., Cai, M.L. and Kuszewski, J. (1999) *J. Am. Chem. Soc.*, **121**, 6513–6514.

Dingley, A.J. and Grzesiek, S. (1998) *J. Am. Chem. Soc.*, **120**, 8293–8297.

Eletsky, A., Heinz, T., Moreira, O., Kienhöfer, A., Hilvert, D. and Pervushin, K. (2002) *J. Biomol. NMR*, **24**, 31–39.

Eletsky, A., Kienhöfer, A. and Pervushin, K. (2001) *J. Biomol. NMR*, **20**, 177–180.

Ernst, M. and Ernst, R.R. (1994) *J. Magn. Reson. Ser.*, **A110**, 202–213.

Ernst, R.R., Bodenhausen, G. and Wokaun, A. (1987) *The Principles of Nuclear Magnetic Resonance in One and Two Dimensions*, Clarendon, Oxford.

Farmer, B.T. and Venters, R.A. (1996) *J. Biomol. NMR*, **7**, 59–71.

Fernandez, C., Adeishvili, K. and Wuthrich, K. (2001a) *Proc. Natl. Acad. Sci. USA*, **98**, 2358–2363.

Fernandez, C., Hilty, C., Bonjour, S., Adeishvili, K., Pervushin, K. and Wüthrich, K. (2001b) *FEBS Lett.*, **504**, 173–178.

Fischer, M.W.F., Zeng, L. and Zuiderweg, E.R.P. (1996) *J. Am. Chem. Soc.*, **118**, 12457– 12458.

Gardner, K.H. and Kay, L.E. (1998) *Annu. Rev. Biophys. Biomol. Struct.*, **27**, 357–406.

Gardner, K.H., Rosen, M.K. and Kay, L.E. (1997) *Biochemistry*, **36**, 1389–1401.

Grzesiek, S., Anglister, J., Ren, H. and Bax, A. (1993) *J. Am. Chem. Soc.*, **115**, 4369–4370.

Guntert, P., Mumenthaler, C. and Wüthrich, K. (1997) *J. Mol. Biol.*, **273**, 283–298.

Hwang, P.M., Choy, W.Y., Lo, E.L., Chen, L., Forman-Kay, J.D., Raetz, C.R., Prive, G.G., Bishop, R.E. and Kay, L.E. (2002) *Proc. Natl. Acad. Sci. USA*, **99**, 13560–13565.

Ikura, M., Kay, L.E., Tschudin, R. and Bax, A. (1990) *J. Magn. Reson.*, **86**, 204–209.

Kadkhodaie, M., Rivas, O., Tan, M., Mohebbi, A. and Shaka, A.J. (1991) **91**, 437–443.

Kay, L.E. and Gardner, K.H. (1997) *Curr. Opin. Struct. Biol.*, **7**, 722–731.

LeMaster, D.M. (1989) *Meth. Enzymol.*, **177**, 23–43.

LeMaster, D.M. (1990a) *Quart. Rev. Biophys.*, **23**, 133–174.

LeMaster, D.M. (1990b) *Annu. Rev. Biophys. Biophys. Chem.*, **19**, 243–266.

Lohr, F. and Ruterjans, H. (2002) *J. Magn. Reson.*, **156**, 10–18.

Machonkin, T.E., Westler, W.M. and Markley, J.L. (2002) *J. Am. Chem. Soc.*, **124**, 3204–3205.

Madi, Z.L., Brutscher, B., Schulte-Herbruggen, T., Bruschweiler, R. and Ernst, R.R. (1997) *Chem. Phys. Lett.*, **268**, 300–305.

Marion, D., Ikura, M., Tschudin, R. and Bax, A. (1989) *J. Magn. Reson.*, **85**, 393–399.

Mulder, F.A.A., Ayed, A., Yang, D.W., Arrowsmith, C.H. and Kay, L.E. (2000) *J. Biomol. NMR*, **18**, 173–176.

Mumenthaler, C., Guntert, P., Braun, W. and Wüthrich, K. (1997) *J. Biomol. NMR*, **10**, 351–362.

Oh, B.H., Westler, W.M., Darba, P. and Markley, J.L. (1988) *Science*, **240**, 908–911.
Pervushin, K. and Eletsky, A. (2003) *J. Biomol. NMR*, **25**, 147–152.
Pervushin, K., Ono, A., Fernandez, C., Szyperski, T., Kainosho, M. and Wuthrich, K. (1998) *Proc. Natl. Acad. Sci. USA*, **95**, 14147–14151.
Pervushin, K., Riek, R., Wider, G. and Wüthrich, K. (1997) *Proc. Natl. Acad. Sci. USA*, **94**, 12366–12371.
Peters, J.A., Huskens, J. and Raber, D.J. (1996) *Prog. Nucl. Magn. Reson. Spectrosc.*, **28**, 283–350.
Pintacuda, G. and Otting, G. (2002) *J. Am. Chem. Soc.*, **124**, 372–373.
Powell, D.H., Ni Dhubhghaill, O.M., Pubanz, D., Helm, L., Lebedev, Y.S., Schlaepfer, W. and Merbach, A.E. (1996) *J. Am. Chem. Soc.*, **118**, 9333–9346.
Reif, B., Hennig, M. and Griesinger, C. (1997) *Science*, **276**, 1230–1233.
Reynolds, W.F. and Enriquez, R.G. (2002) *J. Nat. Prod.*, **65**, 221–244.
Salzmann, M., Pervushin, K., Wider, G., Senn, H. and Wüthrich, K. (1999a) *J. Biomol. NMR*, **14**, 85–88.
Salzmann, M., Wider, G., Pervushin, K., Senn, H. and Wüthrich, K. (1999b) *J. Am. Chem. Soc.*, **121**, 844–848.
Salzmann, M., Pervushin, K., Wider, G., Senn, H. and Wüthrich, K. (2000) *J. Am. Chem. Soc.*, **122**, 7543–7548.
Sass, H.J., Musco, G., Stahl, S.J., Wingfield, P.T. and Grzesiek, S. (2000) *J. Biomol. NMR*, **18**, 303–309.
Schubert, M., Kolbe, M., Kessler, B., Oesterhelt, D. and Schmieder, P. (2002) *Chembiochem*, **3**, 1019–1023.
Shaka, A.J., Keeler, J., Frenkiel, T. and Freeman, R. (1983) *J. Magn. Reson.*, **52**, 335–338.
Sharp, R., Lohr, L. and Miller, J. (2001) *Prog. Nucl. Magn. Reson. Spectrosc.*, **38**, 115–158.
Takahashi, H., Nakanishi, T., Kami, K., Arata, Y. and Shimada, I. (2000) *Nat. Struct. Biol.*, **7**, 220–223.
Tjandra, N. and Bax, A. (1997) *Science*, **278**, 1111–1114.
Tjandra, N., Garrett, D.S., Gronenborn, A.M., Bax, A. and Clore, G.M. (1997a) *Nat. Struct. Biol.*, **4**, 443–449.
Tjandra, N., Omichinski, J.G., Gronenborn, A.M., Clore, G.M. and Bax, A. (1997b) *Nat. Struct. Biol.*, **4**, 732–738.
Tolman, J.R., Flanagan, J.M., Kennedy, M.A. and Prestegard, J.H. (1995) *Proc. Natl. Acad. Sci. USA*, **92**, 9279–9283.
Tugarinov, V., Muhandiram, R., Ayed, A. and Kay, L.E. (2002) *J. Am. Chem. Soc.*, **124**, 10025–10035.
Tycko, R., Blanco, F.J. and Ishii, Y. (2000) *J. Am. Chem. Soc.*, **122**, 9340–9341.
Venters, R.A., Farmer, B.T., Fierke, C.A. and Spicer, L.D. (1996) *J. Mol. Biol.*, **264**, 1101–1116.
Wagner, G. (1993) *J. Biomol. NMR*, **3**, 375–385.
Westler, W.M., Kainosho, M., Nagao, H., Tomonaga, N. and Markley, J.L. (1988) *J. Am. Chem. Soc.*, **110**, 4093–4095.
Wu, Z.R., Tjandra, N. and Bax, A. (2001) *J. Am. Chem. Soc.*, **123**, 3617–3618.
Wüthrich, K. (1986) *NMR of Proteins and Nucleic Acids*, Wiley, New York, NY.
Yang, D.W. and Kay, L.E. (1999) *J. Am. Chem. Soc.*, **121**, 2571–2575.
Zhu, G., Xia, Y.L., Sze, K.H. and Yan, X.Z. (1999) *J. Biomol. NMR*, **14**, 377–381.